doi:10.1016/j.ymthe.2005.07.684

ARTICLE

# Dermal Wound Healing Is Subject to Redox Control

Sashwati Roy,[1] Savita Khanna,[1] Kishore Nallu,[1] Thomas K. Hunt,[2] and Chandan K. Sen[1,*]

[1]*Laboratory of Molecular Medicine, Department of Surgery, Comprehensive Wound Center, Davis Heart & Lung Research Institute, The Ohio State University Medical Center, Columbus, OH 43210, USA*
[2]*Department of Surgery, University of California at San Francisco, San Francisco, CA 94143, USA*

**To whom correspondence and reprint requests should be addressed at 512 DHLRI, OSU, 473 W. 12th Avenue, Columbus, OH 43210, USA. Fax: +1 (614) 247 7818. E-mail: sen-1@medctr.osu.edu.*

Available online 26 August 2005

**Previously we have reported *in vitro* evidence suggesting that that $H_2O_2$ may support wound healing by inducing VEGF expression in human keratinocytes (C. K. Sen *et al.*, 2002, *J. Biol. Chem.* 277, 33284–33290). Here, we test the significance of $H_2O_2$ in regulating wound healing *in vivo.* Using the Hunt–Schilling cylinder approach we present the first evidence that the wound site contains micromolar concentrations of $H_2O_2$. At the wound site, low concentrations of $H_2O_2$ supported the healing process, especially in $p47^{phox}$- and MCP-1-deficient mice in which endogenous $H_2O_2$ generation is impaired. Higher doses of $H_2O_2$ adversely influenced healing. At low concentrations, $H_2O_2$ facilitated wound angiogenesis *in vivo.* $H_2O_2$ induced FAK phosphorylation both in wound-edge tissue *in vivo* and in human dermal microvascular endothelial cells. $H_2O_2$ induced site-specific (Tyr-925 and Tyr-861) phosphorylation of FAK. Other sites, including the Tyr-397 autophosphorylation site, were insensitive to $H_2O_2$. Adenoviral gene delivery of catalase impaired wound angiogenesis and closure. Catalase overexpression slowed tissue remodeling as evidenced by a more incomplete narrowing of the hyperproliferative epithelium region and incomplete eschar formation. Taken together, this work presents the first *in vivo* evidence indicating that strategies to influence the redox environment of the wound site may have a bearing on healing outcomes.**

**Key Words: trauma, hydrogen peroxide, redox signaling, oxygen**

## INTRODUCTION

Disrupted vasculature limits the supply of oxygen to the wound site. Compromised tissue oxygenation or wound hypoxia is viewed as a major factor that limits the healing process as well as wound disinfection [1]. The general consensus is that, at the wound site, oxygen fuels tissue regeneration [2] and that oxygen-dependent respiratory burst is a primary mechanism to resist infection [3]. We postulated that oxygen-derived reactive species at the wound site not only disinfect the wound but contribute directly to facilitating the healing process [4].

Wound healing commences with blood coagulation followed by infiltration of neutrophils and macrophages at the wound site to release reactive oxygen species (ROS) by an oxygen-consuming respiratory burst. In 1999, the cloning of mox1 (later named Nox1) marked a major progress in categorically establishing the presence of distinct NADPH oxidases in nonphagocytic cells [5]. These data taken together, the wound site has two clear sources of ROS: (i) transient delivery of larger amounts by respiratory burst of phagocytic cells and (ii) sustained delivery of lower amounts by enzymes of the Nox/Duox family present in cells such as the fibroblasts, keratinocytes, and endothelial cells. Recent studies show that, at low concentrations, ROS may serve as signaling messengers in the cell and regulate numerous signal transduction and gene expression processes [6]. Inducible ROS generated in some nonphagocytic cells are implicated in mitogenic signaling [7]. A direct role of NADPH oxidases and ROS in facilitating angiogenesis has been proven [8]. In line with these observations we have previously reported that at the wound site, ROS may promote wound angiogenesis by inducing vascular endothelial growth factor (VEGF) expression in wound-related cells such as keratinocytes and macrophages [9]. In this study, we tested the significance of ROS in the healing of experimental dermal wounds.

## RESULTS

### Wound-Site $H_2O_2$: Generation and Significance

We present the first evidence demonstrating that wound fluid contains micromolar concentrations of steady-state $H_2O_2$ (Fig. 1). Of note, we detected $H_2O_2$ levels in both



1525-0016/$30.00

doi:10.1016/j.ymthe.2005.07.684

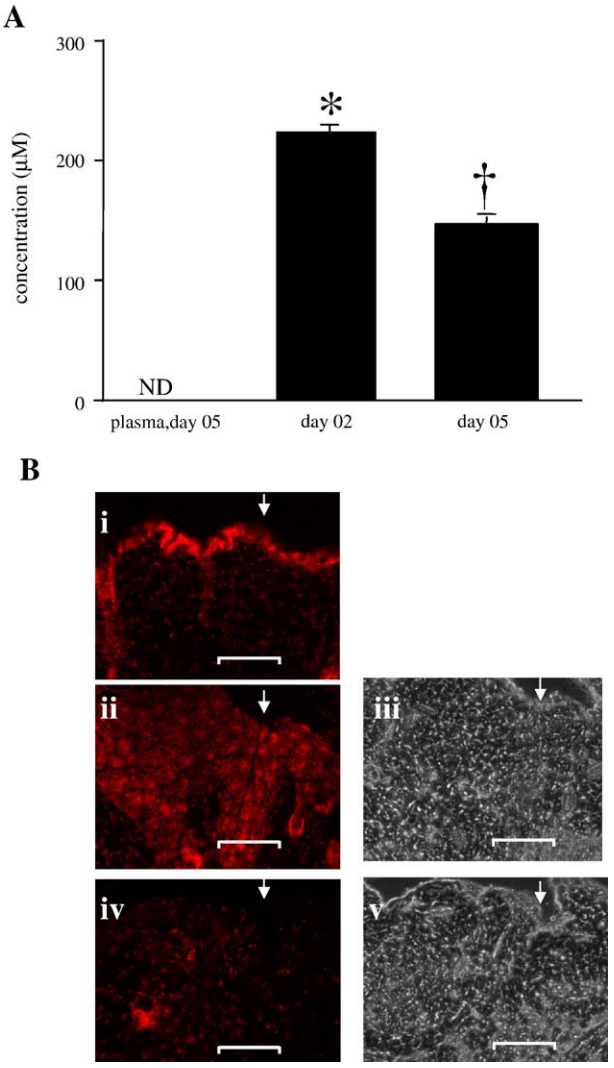


**FIG. 1.** Presence of reactive oxygen species at the wound-site. (A) $H_2O_2$ concentration in wound fluid. Hunt–Schilling cylinders were implanted in each of 10 8- to 10-week-old C57BL/6 mice. On days 2 and 5, fluid was collected. Plasma: even in the presence of 200 mM $NaN_3$ (added to inhibit peroxidase activity) $H_2O_2$ was below detection limits (ND, not detectable). Day 02 and day 05: to discern the $H_2O_2$-sensitive component of the signal detected in wound fluid 0.03 ml of the azide-free fluid was treated with 350 units of catalase. The catalase-sensitive component was interpreted as $H_2O_2$. Standard curve was generated using authentic $H_2O_2$ tested for UV absorbance. $n = 4$, $^*P < 0.01$ compared to plasma value, $\dagger P < 0.01$ compared to day 02. (B) Superoxide production in normal skin and wound edge tissue. The skin or wound edge samples ($n = 3$) were harvested at 12 h after wounding and immediately frozen in OCT. Fresh 30-μm sections were incubated with DHE (0.01 mM, 20 min) to detect $O_2^{\cdot -}$. To demonstrate the specificity of DHE signal, superoxide dismutase (10 U/ml) was added while the wound edge samples were incubating with DHE. (i) DHE (red) signal in excised skin tissue, (ii) DHE signal in dermal wound edge 12 h after wounding, (iii) phase contrast image of ii, (iv) DHE signal in wound edge in the presence of 10 U/ml superoxide dismutase, (v) phase contrast image of iv. Scale bar, 100 μm.

inflammatory and postinflammatory phases, i.e., days 2 and 5 postwounding. In the murine model of full-thickness excisional wounds, macrophage infiltration is known to peak at day 3 postwounding [20]. The $H_2O_2$ levels in the wound fluid were significantly higher during the inflammatory phase (day 2) compared to the postinflammatory phase (day 5). Utilizing enzymatically intact frozen wound-edge tissue sections we compared the superoxide production between intact skin and the edge tissue of the excisional dermal wound. Superoxide production in the wound-edge tissue was markedly more than that generated by the intact skin (Fig. 1B). Next, we sought to determine the functional significance of $H_2O_2$ at the wound site. We observed that topical application of low-dose $H_2O_2$ accelerated wound closure (Fig. 2A). $H_2O_2$ at relatively high concentrations is known to be a wound disinfectant. Thus, we were led to question whether the beneficial effect of $H_2O_2$ was indeed wholly or partly mediated by the ability of $H_2O_2$ to cleanse the wound. Even under the stringent surgical conditions used in our study, a low bacterial load colonized the superficial dermal wound tissue. Importantly, $H_2O_2$ treatment did not affect such infection status. No bacterial infection was noted in the deep wound tissue (Fig. 2B). In surgical practice, the use of a strong solution (3%, v/v) of $H_2O_2$ to cleanse the wound has been common. $H_2O_2$ at high levels is capable of inciting oxidative tissue damage and complicating regeneration of nascent tissue [21]. We observed that, indeed, application of a low volume of 3% $H_2O_2$ to the wound significantly delayed wound closure (Figs. 2C and 2D). The use of an even stronger solution resulted in overt tissue damage, leading to severe injury and death of mice (not shown). Taken together, these findings emphasize the significance of the strength of $H_2O_2$ applied topically to wounds.

### $H_2O_2$-Induced Angiogenic Responses

Simultaneous study of a set of angiogenic genes using the quantitative ribonuclease protection assay approach demonstrated that VEGF and its receptor VEGFR-1 or Flt-1 is rapidly induced in response to healing. The inducible expression of these two genes was clearly specific, rapid, and sustained (Fig. 3A). Topically applied low-dose $H_2O_2$ potentiated wound-induced VEGF and Flt-1 expression in the wound edge (Fig. 3B). Repeated topical treatment of one of the paired excisional dermal wounds improved blood flow (Fig. 3C). Immunohistological studies of the wound-edge tissue for the presence of endothelial cells provided consistent evidence supporting that low-dose $H_2O_2$ treatment was associated with increased abundance of endothelial cells (Fig. 3D) and vascularity (Fig. 3E) at the wound edge.

### $H_2O_2$-Induced Site-Specific Phosphorylation of Focal Adhesion Kinase (FAK)

FAK plays a central role in driving angiogenesis [22]. We observed that FAK phosphorylation is $H_2O_2$ inducible

(Fig. 4A). Upon stimulation, FAK is phosphorylated on six tyrosine residues: Tyr-397, Tyr-407, Tyr-576, Tyr-577, Tyr-861, and Tyr-925 [23]. Each of these sites has a specific functional significance and is subject to site-specific phosphorylation [24]. Tyr-925 phosphorylation of FAK within focal adhesions is known to support angiogenic responses [25]. In human dermal microvascular endothelial cells (HMEC), the Tyr-925 and Tyr-861 sites were specifically phosphorylated in the presence of low concentrations of $H_2O_2$ (Fig. 4B). $H_2O_2$ also induced FAK phosphorylation in the wound edge *in vivo* (Fig. 4C).

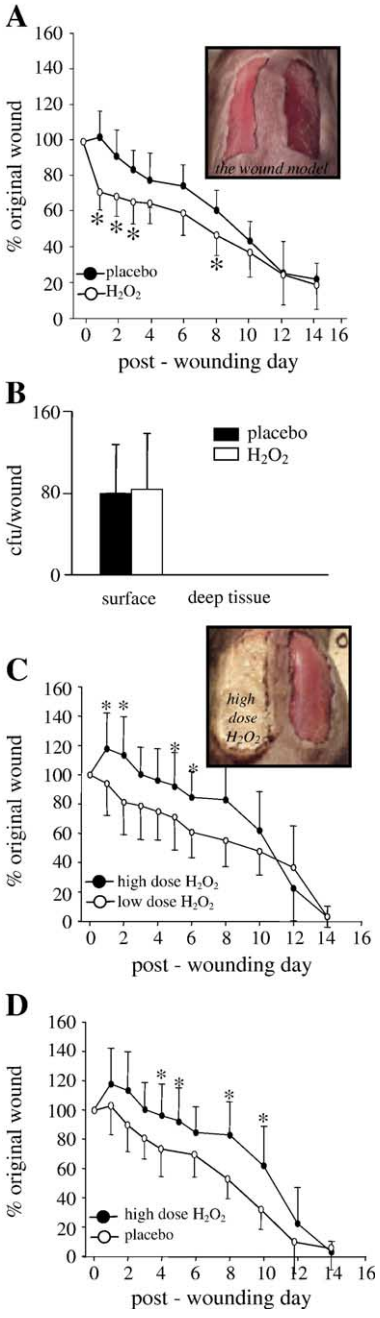


**FIG. 2.** Topical $H_2O_2$ and wound closure. Two 8 × 16-mm full-thickness excisional wounds (A, inset, day 0) were made on the dorsal skin of mice. Each of the two wounds was topically treated with either $H_2O_2$ or saline. (A) Low dose of $H_2O_2$ (1.25 μmol/wound, or 0.025 ml of 0.15% or 50 mM solution/wound, once daily, days 0–4) treatment facilitated closure moderately compared to placebo saline-treated side. $n = 6$, $^*P < 0.05$. (B) Low dose $H_2O_2$ treatment does not influence wound microflora. For determination of surface microflora, wounds (treated with either 1.25 μmol $H_2O_2$/wound or saline) were swabbed (24–48 h postwounding. For deep tissue wound microflora, 48 h after wounding eschar tissue was removed, wound bed tissue underneath the eschar was sampled, and quantitative assessment of bacterial load was performed. Values shown represent means ± SD of CFU of three observations. (C) High dose (25 μmol/wound, or 0.025 ml of 3% solution) versus low (1.25 μmol/wound, or 0.025 ml of 0.15%), once daily on days 0–4, of $H_2O_2$ adversely affected closure. $^*P < 0.05$; compared to low-dose $H_2O_2$ treatment. (D) Comparison of the outcomes of high-dose $H_2O_2$ treatment (C) with those of placebo-treated wounds (A) in different mice. Compared to placebo saline (once daily on days 0–4) treatment, high dose $H_2O_2$ (0.025 ml of 3% $H_2O_2$) adversely affected closure. $n = 6$, $^*P < 0.05$.

### Physiological $H_2O_2$-Delivery Systems

Mice are very aggressive healers, closing dermal defects as large as over 10% of their total body surface within 2 weeks' time [9]. Thus, it is apparent that the basal healing machinery is highly efficient, leaving little room for further acceleration of healing in wild-type mice. Dermal wounding results in rapid induction of genes encoding chemokines that recruit inflammatory cells to the wound site (Fig. 5A). Specific genetically altered mice that suffer from impaired healing serve as useful models to study the effects of agents that may promote wound closure and healing. Monocyte chemotactic protein-1 (MCP-1)-deficient mice suffer from impaired wound angiogenesis and healing [26]. In tissues, macrophages are known to be significant producers of $H_2O_2$ by the NADPH oxidase-dependent respiratory burst mechanism [27]. We hypothesized that insufficient $H_2O_2$ production at the wound site of MCP-1-deficient mice was one factor that compromised wound angiogenesis and healing. Indeed, treatment of excisional dermal wounds in MCP-1-deficient mice with low-dose $H_2O_2$ completely corrected the rate of wound closure (Fig. 5B).

NADPH oxidase is a key source of $H_2O_2$ in inflammatory cells [27]. A defect in the expression of any of the essential subunits of NADPH oxidase, e.g., $p47^{phox}$, is expected to compromise respiratory burst-dependent oxidant production. Mutations in $p47^{phox}$ are a cause of chronic granulomatous disease (CGD), an immune-deficient condition characterized by an impaired healing response, in humans [28]. Consistently, $p47^{phox}$-deficient mice suffer from impaired healing. The abnormal wound closure in $p47^{phox}$-deficient mice was completely corrected in response to low-dose topical $H_2O_2$ treatment (Fig. 5C). Keratin 14 supports epidermal differentiation and regeneration [29] and its expression is

doi:10.1016/j.ymthe.2005.07.684

triggered by dermal wounding [30]. In intact skin, keratin 14 is present as a narrow margin in the basal layer epidermis, whereas in healing tissue keratin 14 is expressed as a broader band at the hyperproliferative epithelium [30]. Postclosure sampling of regenerated skin from the wound site of $p47^{phox}$-deficient mice revealed that not only did the low-dose $H_2O_2$-treated side close faster but the regenerated skin resembled the keratin 14 distribution in intact skin. In contrast, the regenerated skin of the placebo saline-treated side showed signs of incomplete healing at a matched time point (Fig. 5D).

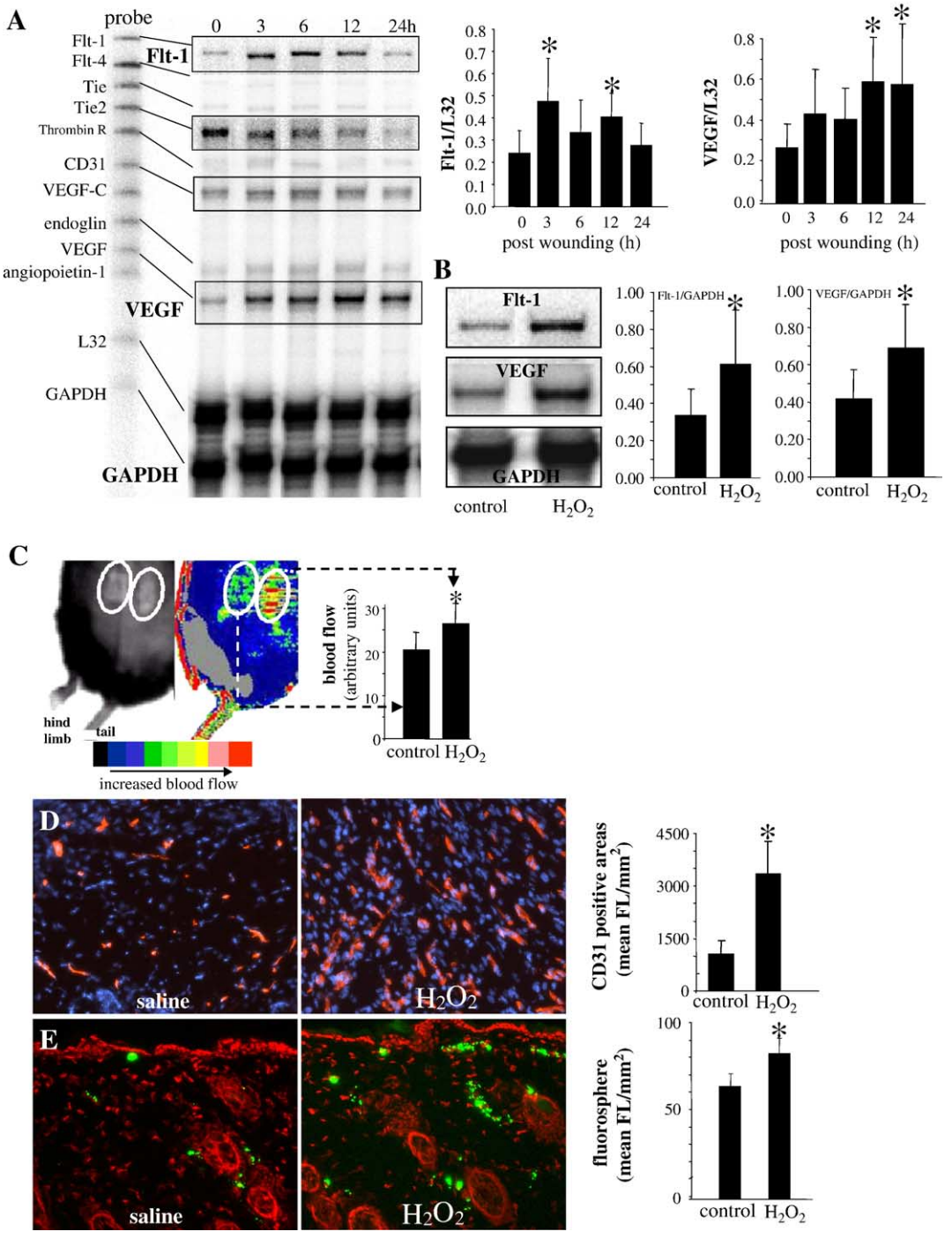

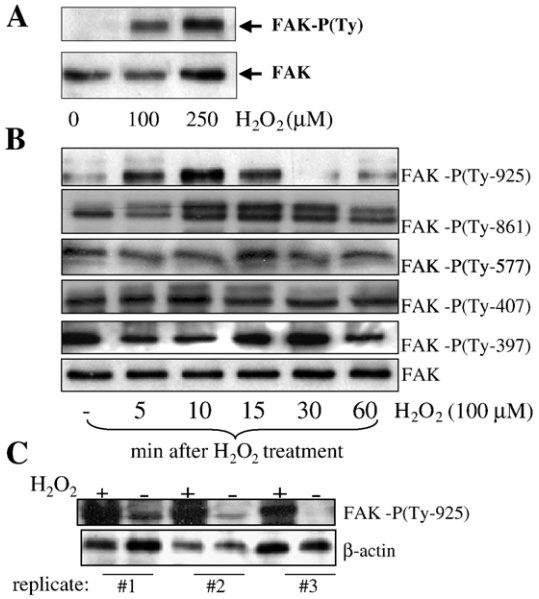


**FIG. 4.** $H_2O_2$-induced phosphorylation of focal adhesion kinase (FAK) in microvascular endothelial cells and wound edge tissue. HMEC-1 were treated with $H_2O_2$ for the indicated dose and duration ($n$ = 3). Phosphorylation of FAK was detected using Western blot and phosphorylation-site-specific antibodies against FAK. Native FAK was blotted to show equal loading. (A) Effect of dose of $H_2O_2$ treatment on phosphorylation (Tyr-925) state of FAK. (B) Kinetics of site-specific phosphorylation of FAK in HMEC cells following $H_2O_2$ (0.1 mM) treatment. (C) Paired excisional wounds (Fig. 2) were treated with either placebo saline or $H_2O_2$ (1.25 μmol/wound). Wound-edge tissue ($n$ = 3) was collected 30 min after wounding.

### Decomposition of Endogenous Wound-Site $H_2O_2$ Impairs Wound Healing

*In vivo* catalase gene transfer represents one productive approach to down-regulating tissue $H_2O_2$ levels [31]. Overexpression of catalase (Fig. 6A) down-regulated inducible early phase VEGF expression at the wound edge (Fig. 6B), consistent with our observations that $H_2O_2$ is a potent and prompt inducer of VEGF both *in vitro* [9] and *in vivo* (Fig. 3B). Such early phase effect of catalase expression did impair wound angiogenesis on a long-term basis. AdCat-treated wound tissues had compromised blood flow (Fig. 6C) compared to the AdLacZ-treated control wounds. Impairment of wound angiogenesis caused by catalase overexpression clearly limited wound closure (Fig. 6D) comparable to the kinetics of wound closure in $p47^{phox}$-deficient mice (Fig. 5C). Histological analysis of wound-edge tissue by trichrome staining substantiated not only that catalase overexpression limited angiogenesis and slowed wound closure but also that the quality of regenerating tissue was distinctly affected. Catalase overexpression slowed tissue restructuring as evident by a more incomplete narrowing [9] of the hyperproliferative epithelium zone and incomplete eschar formation in the time-matched postheal tissue (Fig. 6E).

## Discussion

Interest in the role of oxygen in wound healing spiked when Jacques Cousteau's divers had anecdotally reported that they healed their work wounds significantly better when they lived in an undersea habitat about 35 feet under the surface of the Red Sea [32]. Research during the past 4 decades led to the consensus that limited supply of oxygen to the wound site represents a key limiting factor for healing. More recent research during the past decade substantiate that, in biological tissues, oxygen generates reactive derivatives commonly referred to as reactive oxygen species. While earlier works primarily focused on the damaging aspects of excess ROS, current research builds a compelling case supporting the role of ROS as diffusible signaling messengers [6]. The phagocytic (phox) and nonphagocytic (Nox) NADPH oxidases represent one of the most significant sources of deliberate ROS production in biological tissues. Respiratory burst in phagocytic cells results in transient generation of excess ROS designed to kill pathogens [4]. In contrast, Nox generates low levels of ROS in fibroblasts on a sustained basis to drive a wide variety of biological processes, including angiogenesis [33]. This work provides the first estimation of ROS concentration at the wound site *in vivo*. Our observation that the wound site is enriched in $H_2O_2$ is consistent with previous observations in plants

**FIG. 3.** Wound- and $H_2O_2$-induced changes in angiogenesis-related genes, vascularization, and wound-edge blood flow. Paired excisional wounds (Fig. 2) were treated with either placebo saline or $H_2O_2$ (1.25 μmol/wound, days 0–4, once daily). (A) Ribonuclease protection assay showing kinetics of angiogenesis-related mRNA expression in a placebo saline-treated wound. Densitometry data (means ± SD, $n$ = 4) are shown for Flt-1 and VEGF. *$P < 0.05$ compared to 0 h. (B) Low-dose $H_2O_2$ treatment (1.25 μmol/wound, once at day 0) to wounds further augmented wound-induced Flt-1 and VEGF mRNA expression as determined from wound-edge tissue harvested 6 h after wounding and $H_2O_2$ treatment. Densitometry data (means ± SD, $n$ = 4) are shown. *$P < 0.05$ compared to control. (C) Blood flow imaging of wounds was performed noninvasively using laser Doppler. An image reflecting the blood flow (right) and a digital photo (region of interest; left) from postheal (1 day after complete wound closure) tissue are shown. Means ± SD ($n$ = 3) are presented (bar graph; *$P < 0.05$). (D) Day 8 postwounding, the wound edge was cryosectioned and vascularization was estimated by staining for CD31 (red, rhodamine) and DAPI (blue, nuclei); the higher abundance of CD31 red stain in the section obtained from the $H_2O_2$-treated side (right) demonstrates better vascularization versus control (left). Bar graph presents image analysis outcome (means ± SD, $n$ = 3). *$P < 0.05$ compared to control. (E) Before sacrifice of mice on day 8 postwounding, space-filling carboxylate-modified fluorescent microspheres were injected into the left ventricle of the beating heart to visualize neovascularization in the healing wound. Cryosections (10 μm) fixed in acetone and stained with DAPI (nuclei, shown here in contrast red) were analyzed by fluorescence microscopy. The appearance of the green microspheres at the wound edge represents wound vascularity. Bar graph presents image analysis outcome (means ± SD, $n$ = 3). *$P < 0.05$ compared to control.

doi:10.1016/j.ymthe.2005.07.684

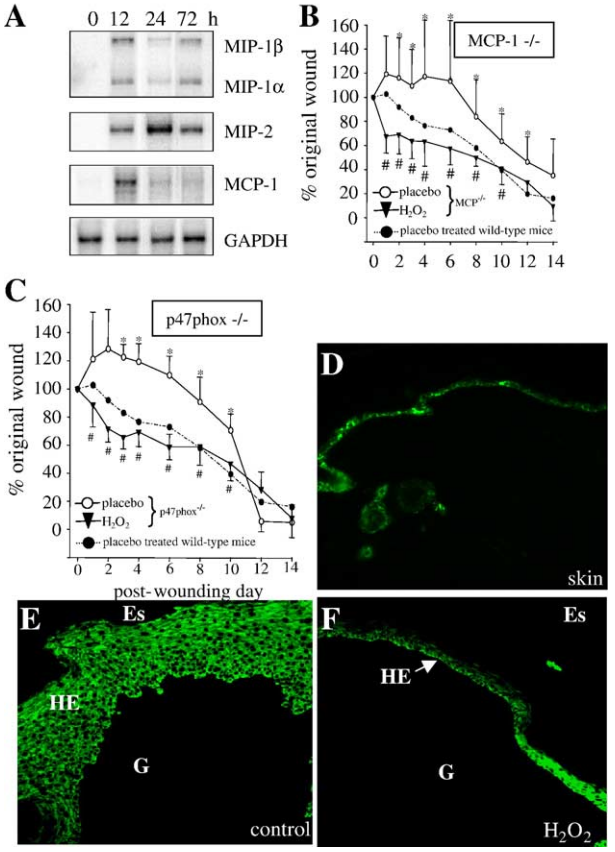


**FIG. 5.** Role of $H_2O_2$ in MCP-1- and p47$^{phox}$-deficient mice. Two excisional wounds (Fig. 2) were made on the dorsal skin of wild-type, MCP-1$^{-/-}$, or p47$^{phox\ -/-}$ mice. Each of the two wounds was treated with either saline or $H_2O_2$ (1.25 μmol/wound; days 0–4). (A) RPA showing kinetics of monocyte/macrophage chemotactic protein-related mRNA expression in placebo saline-treated wounds of wild-type mice ($n = 3$). (B) Wound closures in saline-treated wounds of C57BL/6 mice and $H_2O_2$- or saline-treated MCP-1$^{-/-}$ mice are shown. $n = 7$, $^*P < 0.05$ compared to C57BL/6 saline treatment. $\#P < 0.05$ compared to KO saline treatment. (C) Wound closures in saline-treated wounds of C57BL/6 mice and $H_2O_2$- or saline-treated wounds of p47$^{phox}$ KO mice are shown. $^*P < 0.05$; compared to C57BL/6 saline treatment. $\#P < 0.05$ compared to KO saline treatment. (D) Keratin 14 (green fluorescence) expression in murine skin. (E and F) Keratin 14 expression in skin of p47$^{phox}$ KO mice harvested from wound sites after closure on day 18 postwounding. Note higher expression of keratin 14 in control side (E) compared to $H_2O_2$-treated side (F), indicating healing is ongoing on the control side, while the $H_2O_2$-treated side shows keratin 14 expression comparable to that of normal skin (D). For orientation (see histological identifying characteristics in Fig. 6C): Es, eschar; G, granulation tissue; HE, hyperproliferative epithelium.

recording that endogenous $H_2O_2$ levels increase in wounded leaves [34].

The wound site starts to be occupied by the granulation tissue approximately 4 days after injury. New capillaries primarily contribute to the granular appearance. Macrophages, fibroblasts, and blood vessels are major components of the granulation tissue. Guided by products contributed by macrophages wound angiogenesis picks up its pace. Basic fibroblast growth factor (FGF2) and VEGF are two key facilitators of wound angiogenesis. Other growth factors such as platelet-derived growth factor, TGF-β, and insulin-like growth factor 1 prepare the fibroblasts to participate in the formation of granulation tissue [4]. $H_2O_2$ enhances the affinity of FGF2 for its receptor [35]. In addition, ROS induce FGF2 expression [36]. $H_2O_2$ induces VEGF expression in wound-related cells [9]. VEGF is believed to be the most prevalent, efficacious, and long-term signal that is known to stimulate angiogenesis in wounds [37]. Recently it has been demonstrated that Nox1-derived ROS is a potent trigger of the angiogenic switch, increasing vascularity and inducing molecular markers of angiogenesis. Nox1 also induces matrix metalloproteinase activity, another marker of the angiogenic switch. Nox1-dependent induction of VEGF is eliminated by coexpression of catalase, indicating that $H_2O_2$ signals for the switch to the angiogenic phenotype [33]. Vascular endothelial growth factor receptors are considered essential for angiogenesis. The VEGFR-family proteins consist of VEGFR-1/Flt-1, VEGFR-2/KDR/Flk-1, and VEGFR-3/Flt-4. In contrast to VEGF and its receptor VEGFR-2, placental growth factor and its receptor VEGFR-1 have been largely neglected. VEGFR-1 plays an important role in the angiogenic switch. VEGFR-1 or Flt-1 is effective in the growth of new and stable vessels in cardiac and limb ischemia through its action on endothelial, smooth muscle, and inflammatory cells and their precursors [38]. Our results indicate that the expression of VEGFR-1 in the wound-edge tissue is sensitive to low-dose $H_2O_2$ treatment. This observation is consistent with the report demonstrating that the expression of VEGFR-1/Flt-1 is highly induced in $H_2O_2$-rich vascular cells in Nox1-expressing tumors [33].

FAK is a positive regulator of both cell motility and cell survival and may contribute to the development of a stable neovasculature. FAK signaling results from its ability to become highly phosphorylated in response to external stimuli. The major site of autophosphorylation, tyrosine 397, is a docking site for the SH2 domains of Src family proteins. The other sites of phosphorylation are phosphorylated by Src kinases. We observed that both in HMEC and in the wound-edge tissue, tyrosine 925 in FAK is specifically phosphorylated in response to low-dose $H_2O_2$. This observation is consistent with the established finding that c-Src kinase activity is $H_2O_2$ inducible [39]. FAK is subject to site-specific phosphorylation [24]. Our observation that $H_2O_2$-induced phosphorylation of FAK is site specific is in agreement. Previously it has been reported that stimulation of FAK by low-density lipoprotein results in specific phosphorylation of Tyr-925, surpassing the phosphorylation of the other residues, including Tyr-397 [24]. Our studies with HMEC point toward Tyr-925 and Tyr-861 as being sensitive to $H_2O_2$. Indeed, site-specific phosphorylation of FAK at the 861 and 925 Tyr sites has been observed to share common

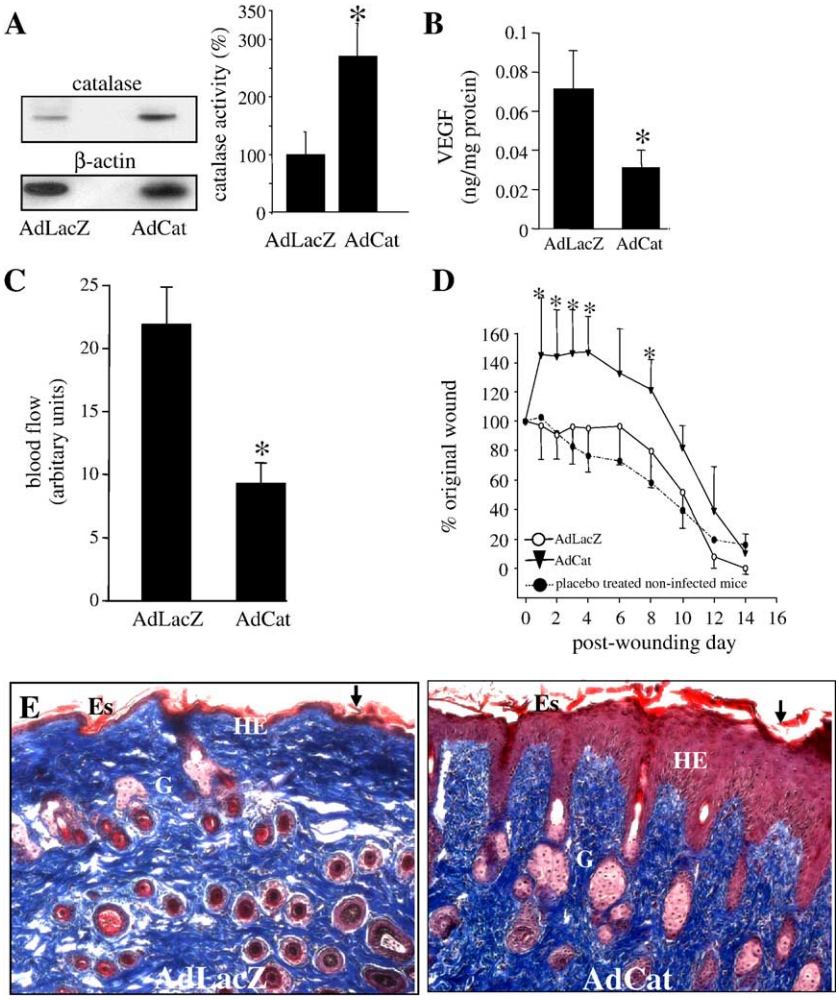


**FIG. 6.** Catalase overexpression impairs healing. (A) Western blot of infected ($10^{11}$ CFU) skin showing catalase overexpression in the side treated with AdCatalase (AdCat) virus compared to the side treated with control AdLacZ virus. Blots were reprobed with β-actin to confirm equal loading of samples. Activity assay demonstrated that the AdCat approach was effective in significantly (*$P < 0.05$) increasing catalase activity in the tissue compared to the AdLacZ control. (B) VEGF protein expression in wound edge on day 1 postwounding. (C) Blood flow at the wound site on day 6 postwounding. Blood flow imaging of wounds was performed noninvasively using a laser Doppler blood flow imaging device as described in the legend to Fig. 3C. (D) Dotted line represents standard healing curve of saline-treated C57BL/6 mice without viral infection. *$P < 0.05$ compared to LacZ-treated side. (E) Masson trichrome staining was performed on formalin-fixed paraffin sections of regenerated skin at the wound site sampled on the day both wounds closed. AdCat side (right) shows broader HE region indicative of incomplete (vs control on left) regeneration of skin, consistent with slower closure. The wound edge is marked with an arrow. Es, eschar; G, granulation tissue; HE, hyperproliferative epithelium.

mechanisms [40]. Activation of FAK may support angiogenesis by a number of mechanisms, including the formation of actin stress fibers/focal adhesions [41], strengthening of the endothelial barrier [42], facilitating VEGF signaling [43,44], and mediating integrin-sensitive signaling pathways [23]. Recently, direct proof that vascular defects in $FAK^{-/-}$ mice result from the inability of FAK-deficient endothelial cells to organize themselves into vascular networks was reported [22].

Just hours after injury, the wound site recruits inflammatory cells. MCP-1-deficient mice recruit fewer phagocytic macrophages to the injury site [45]. In addition, the macrophages that are recruited suffer from compromised functionality [26]. MCP-1 is angiogenic *in vivo* [46]. At the wound site, macrophages deliver numerous angiogenic products [47], including $H_2O_2$ [27]. Our observation that impairment of dermal wound healing in MCP-1-deficient mice [26] may be completely abrogated by topical low-dose $H_2O_2$ treatment points toward a central role for inflammatory cell-derived $H_2O_2$ in promoting wound closure. Supporting data from experiments with mice containing defective NADPH oxidase, the primary enzyme responsible for $H_2O_2$ generation by inflammatory cells, lend additional strength to the notion that endogenously generated $H_2O_2$ at the wound site is a key factor in wound healing. Mutations in $p47^{phox}$ are a cause of CGD in humans. CGD is an immune-deficient condition characterized by impaired healing response [28]. The $p47^{phox\ -/-}$ mouse exhibits a phenotype similar to that of human CGD [48]. $p47^{phox}$ deficiency impairs NADPH oxidase-dependent $H_2O_2$ formation [49]. We have observed that wild-type mice are capable of generating significant amounts of $H_2O_2$ at the wound site. Thus, the beneficial effects of additional topical $H_2O_2$ in such mice were only modest. However, in $p47^{phox}$-deficient mice suffering from compromised ability to generate wound-site $H_2O_2$ the effects of topical 0.15% $H_2O_2$ were more striking. *In vivo* catalase gene

doi:10.1016/j.ymthe.2005.07.684

transfer is one approach by which the effects of endogenous $H_2O_2$ are assessed. Catalase-dependent removal of endogenous $H_2O_2$ at the wound site resulted in a clear adverse effect on the healing outcome. This observation, taken together with the result that topical $H_2O_2$ facilitates dermal wound healing, points toward a clear role for $H_2O_2$ as a messenger for dermal wound healing.

Over the counter, $H_2O_2$ is commonly available at a strength of 3%. Historically, at such strength $H_2O_2$ has been clinically used for disinfection of tissues [50]. The use of $H_2O_2$ to disinfect wounds continues today with a valid concern that at such high doses $H_2O_2$ may hurt nascent regenerating tissues [21]. Indeed, we observed no beneficial effect of 3% $H_2O_2$. This work presents the first evidence suggesting that at the wound site, low levels of $H_2O_2$ are generated. At such micromolar levels, $H_2O_2$ drives redox-sensitive signaling mechanisms. Although the current work focuses on $H_2O_2$-sensitive mechanisms underlying wound angiogenesis, it is important to note that redox-sensitive mechanisms may influence numerous aspects of dermal wound healing [4]. Topical application of 0.15% $H_2O_2$ favorably influenced wound angiogenesis. Chronic wounds are typically hypoxic and thus limited in their ability to generate endogenous $H_2O_2$. In addition, CGD patients are clearly impaired in their ability to generate endogenous $H_2O_2$. For such cases, therapeutic strategies based on targeting the wound-site redox state may deliver.

## MATERIALS AND METHODS

### Materials

AdLacZ and AdCatalase viral vectors were provided by Dr. John F. Engelhardt of Iowa University. CDC-HMEC-1 cells (SV40 T antigen-transformed human microvascular endothelial cells) were provided by the Centers for Disease Control (Atlanta, GA, USA) [10]. The $p47^{phox}$ KO mice were provided by Dr. S. Holland, NIAID, NIH, and MCP-$1^{-/-}$ mice were obtained from Dr. B. J. Rollins (Mount Sinai School of Medicine, New York, NY, USA). Unless otherwise stated all other chemicals and reagents were obtained from Sigma Chemical Co. (St. Louis, MO, USA) and were of the highest grade available.

### Secondary-Intention Excisional Dermal Wound Model

Young male (8 weeks of age) C57BL/6 mice were used. Two 8 × 16-mm full-thickness excisional wounds [9] were placed on the dorsal skin, equidistant from the midline and adjacent to the four limbs (Fig. 2). The animals were killed at the indicated times and wound edges were collected for analyses. For wound-edge harvest, 1–1.5 mm of the tissue from the leading edge of the wounded skin was excised around the entire wound.

***Hunt–Schilling cylinder for wound fluid collection.*** The implantation of a wire mesh cylinder (stainless steel; 2.5-cm length and 0.8-cm diameter) and wound fluid harvest were performed as described previously [11]. While this approach is a powerful tool to investigate wound fluid composition, most studies have used it for wound fluid studies with time points of 1 to 3 weeks following implantation. This is because of limitations in the volume of wound fluid available for harvest at earlier time points. We have standardized techniques to harvest wound fluid as soon as day 2 after implantation.

***Catalase gene transfer.*** Because of potential hazards involved in viral gene delivery to open wounds, intact skin in each of the two wound sites was subcutaneously injected ($10^{11}$ CFU) using a Hamilton gas-tight syringe with a 28-gauge needle [12] with either AdCat (catalase) or AdLacZ (control) 5 days prior to wounding. All animal protocols were approved by the Institutional Lab Animal Care and Use Committee of the Ohio State University.

***Determination of wound area.*** Imaging of wounds was performed using a digital camera (Mavica FD91, Sony). The wound area was determined using WoundMatrix software as described previously [9].

### ROS Detection in Wounds

***$O_2^{\bullet -}$ detection.*** Freshly frozen, enzymatically intact, 30-μm-thick sections of wound edge were incubated with DHE (10 μM) in PBS for 30 min at 37°C protected from light. DHE, oxidized to ethidium, was detected using a confocal microscope equipped with a 543-nm He–Ne laser and 560-nm long-pass filter [13]. This approach has been effectively utilized to test superoxide production in intact tissue sections, which in turn may also be interpreted as a measure of NADPH oxidase in the tissue [13].

***Direct $H_2O_2$ measurements.*** $H_2O_2$ levels in wound fluid were measured using a real-time electrochemical $H_2O_2$ measurement as described [14]. The Apollo 4000 system (WPI, Sarasota, FL, USA) was used for analysis. $H_2O_2$ was measured using the ISO-HPO-2 2.0-mm stainless steel sensor, with replaceable membrane sleeves and an internal refillable electrolyte. This electrode technology includes a $H_2O_2$-sensing element and separate reference electrode encased within a single Faraday-shielded probe design (WPI). Catalase-sensitive signal provided a measure of $H_2O_2$.

### Assessment of Microbial (Bacterial) Growth in Wounds

***Superficial bacterial load.*** Twenty-four or 48 h after wounding, the surface was swabbed for 20 s using an alginate-tipped applicator. Serial dilution of quantitative swabs was performed and plated on sterile agar medium. After 24 h at 37°C in air, the plates were examined and colonies were counted [15].

***Deep tissue bacterial load.*** The superficial eschar tissue was removed. The wound-bed tissue underneath the eschar was excised aseptically, weighed, homogenized, serially diluted, and cultured on agar plates as described above [16].

### Cells and Cell Culture

HMEC-1 were cultured in MCDB-131 growth medium (GIBCO BRL) supplemented with 10% FBS, 100 IU/ml penicillin, 0.1 mg/ml streptomycin, 2 mol/L L-glutamine [17].

### RNase Protection Assay

Total RNA was isolated from wound-edge tissue and snap frozen in liquid nitrogen using Trizol reagent according to standard instructions provided by the manufacturer (Gibco BRL). RNase protection assay was performed utilizing DNA templates from BD Pharmingen (BD RiboQuant; San Diego, CA, USA) and standard procedures [9].

### Wound-Site Functional Angiogenesis

***Wound vascularity.*** Before sacrifice of mice, space-filling carboxylate-modified fluorescent microspheres (FluoSpheres, 0.2 μm, $10^{12}$ particles/ml) were injected into the left ventricle of the beating heart [18]. Wound-edge tissues were embedded in OCT. Cryosections (10 μm) fixed in acetone were analyzed by fluorescence microscopy.

***Blood flow imaging.*** The MoorLDI-Mark 2 laser Doppler blood perfusion imager (Moor Instruments Ltd., UK) was used to map tissue blood flow.

### Protein Analyses

Wound-edge tissue was ground in liquid nitrogen and homogenized using a Teflon homogenizer in ice-cold RIPA lysis buffer containing protease inhibitor cocktail (Sigma) and 1 mM $Na_3VO_4$. The homogenate was

centrifuged at 16,000*g* at 4°C for 15 min. The supernatant was collected for further analyses. For preparation of cytosolic protein extract from monolayer cells, the culture medium was aspirated and replaced by ice-cold phosphate-buffered saline. Monolayers were scraped using a cell lifter. The lifted cells were centrifuged at 4500*g* for 5 min at 4°C. After the supernatant was aspirated, RIPA lysis buffer containing protease inhibitor cocktail and 1 mM $Na_3VO_4$ was added to the pellet. The suspension was vortexed and centrifuged for 10 min at 16,000*g*. The supernatant cytosolic extract was frozen at −80°C for further analyses. For catalase, FAK, and phospho-FAK immunoblots, wound-edge tissue protein extract or cellular cytosolic extracts were separated on a 10% SDS–polyacrylamide gel under reducing conditions, transferred to nitrocellulose, and probed with anti-catalase (1:30,000; Rockland, Gilbertsville, PA, USA), anti-FAK (1:1000 dilution; Upstate Biotech, Lake Placid, NY, USA), or anti-site-specific phospho-FAK antibody (1:1000 dilution; Upstate Biotech). VEGF protein expression was determined using ELISA [9]. Catalase activity was assayed by monitoring the loss of absorbance of $H_2O_2$ at 240 nm. An extinction coefficient of 39.4 $M^{-1}$ $cm^{-1}$ was used for calculation of enzyme activity [19].

### Histology

Formalin-fixed wound edges embedded in paraffin were sectioned. The sections (4 μm) were stained with hematoxylin and eosin using standard procedures or immunostained with the following primary antibodies: keratin14 (1:500; Covance, Berkeley, CA, USA) or CD31 (1:200; BD Pharmingen). To enable fluorescence detection, sections were incubated with the appropriate Alexa Fluor 488- (Molecular Probes, Eugene, OR, USA) conjugated secondary antibody (1:250 dilution).

### Fluorescence Image Analyses

Tissue sections were analyzed by fluorescence microscopy (Axiovert 200M, Zeiss, Germany). Image analysis software (Axiovision 4.3, Zeiss, Germany) was used to quantitate fluorescence intensity (fluorescent pixels) of CD31 or fluorosphere positive areas (expressed as per $mm^2$ area).

### Statistics

*In vitro* data are reported as means ± SD of at least three experiments. *In vivo* data from one wound of a mouse was compared to the other wound on the same mouse using paired *t* test. Comparisons among multiple groups were made by analysis of variance. $P < 0.05$ was considered statistically significant.

## ACKNOWLEDGMENTS

*This work was supported by NIH RO1 GM69589 to C.K.S. Thanks to Drs. Srikanth Pendyala and Subhasis Banerjee for technical assistance.*

RECEIVED FOR PUBLICATION APRIL 13, 2005; REVISED JULY 7, 2005; ACCEPTED JULY 10, 2005

## REFERENCES

1. Gordillo, G. M., and Sen, C. K. (2003). Revisiting the essential role of oxygen in wound healing. *Am. J. Surg.* **186:** 259–263.
2. Kivisaari, J., Vihersaari, T., Renvall, S., and Niinikoski, J. (1975). Energy metabolism of experimental wounds at various oxygen environments. *Ann. Surg.* **181:** 823–828.
3. Grief, R., Akca, O., Horn, E. P., Kurz, A., and Sessler, D. I. (2000). Supplemental perioperative oxygen to reduce the incidence of surgical-wound infection. Outcomes Research Group. *N. Engl. J. Med.* **342:** 161–167.
4. Sen, C. K. (2003). The general case for redox control of wound repair. *Wound Repair Regen.* **11:** 431–438.
5. Suh, Y. A., *et al.* (1999). Cell transformation by the superoxide-generating oxidase Mox1. *Nature* **401:** 79–82.
6. Rhee, S. G. (1999). Redox signaling: hydrogen peroxide as intracellular messenger. *Exp. Mol. Med.* **31:** 53–59.
7. Irani, K., *et al.* (1997). Mitogenic signaling mediated by oxidants in Ras-transformed fibroblasts. *Science* **275:** 1649–1652.
8. Stone, J. R., and Collins, T. (2002). The role of hydrogen peroxide in endothelial proliferative responses. *Endothelium* **9:** 231–238.
9. Sen, C. K., Khanna, S., Babior, B. M., Hunt, T. K., Ellison, E. C., and Roy, S. (2002). Oxidant-induced vascular endothelial growth factor expression in human keratinocytes and cutaneous wound healing. *J. Biol. Chem.* **277:** 33284–33290.
10. Ades, E. W., *et al.* (1992). HMEC-1: establishment of an immortalized human microvascular endothelial cell line. *J. Invest. Dermatol.* **99:** 683–690.
11. Bentley, J. P., *et al.* (1990). Peptides from live yeast cell derivative stimulate wound healing. *Arch. Surg.* **125:** 641–646.
12. Ozawa, K., *et al.* (2001). Expression of the oxygen-regulated protein ORP150 accelerates wound healing by modulating intracellular VEGF transport. *J. Clin. Invest.* **108:** 41–50.
13. Sorescu, D., *et al.* (2002). Superoxide production and expression of nox family proteins in human atherosclerosis. *Circulation* **105:** 1429–1435.
14. Liu, X., and Zweier, J. L. (2001). A real-time electrochemical technique for measurement of cellular hydrogen peroxide generation and consumption: evaluation in human polymorphonuclear leukocytes. *Free Radical Biol. Med.* **31:** 894–901.
15. Bill, T. J., Ratliff, C. R., Donovan, A. M., Knox, L. K., Morgan, R. F., and Rodeheaver, G. T. (2001). Quantitative swab culture versus tissue biopsy: a comparison in chronic wounds. *Ostomy Wound Manage.* **47:** 34–37.
16. Bowler, P. G., Duerden, B. I., and Armstrong, D. G. (2001). Wound microbiology and associated approaches to wound management. *Clin. Microbiol. Rev.* **14:** 244–269.
17. Mason, J. C., Yarwood, H., Sugars, K. B., Morgan, P., Davies, K. A., and Haskard, D. O. (1999). Induction of decay-accelerating factor by cytokines or the membrane-attack complex protects vascular endothelial cells against complement deposition. *Blood* **94:** 1673–1682.
18. Jacobi, J., Jang, J. J., Sundram, U., Dayoub, H., Fajardo, L. F., and Cooke, J. P. (2002). Nicotine accelerates angiogenesis and wound healing in genetically diabetic mice. *Am. J. Pathol.* **161:** 97–104.
19. Aebi, H. (1984). Catalase in vitro. *Methods Enzymol.* **105:** 121–126.
20. DiPietro, L. A., Burdick, M., Low, Q. E., Kunkel, S. L., and Strieter, R. M. (1998). MIP-1alpha as a critical macrophage chemoattractant in murine wound repair. *J. Clin. Invest.* **101:** 1693–1698.
21. Branemark, P. I., and Ekholm, R. (1967). Tissue injury caused by wound disinfectants. *J. Bone Joint Surg. Am. Vol.* **49:** 48–62.
22. Ilic, D., *et al.* (2003). Focal adhesion kinase is required for blood vessel morphogenesis. *Circ. Res.* **92:** 300–307.
23. Cary, L. A., and Guan, J. L. (1999). Focal adhesion kinase in integrin-mediated signaling. *Front. Biosci.* **4:** D102–D113.
24. Relou, I. A., Bax, L. A., van Rijn, H. J., and Akkerman, J. W. (2003). Site-specific phosphorylation of platelet focal adhesion kinase by low-density lipoprotein. *Biochem. J.* **369:** 407–416.
25. Shono, T., Kanetake, H., and Kanda, S. (2001). The role of mitogen-activated protein kinase activation within focal adhesions in chemotaxis toward FGF-2 by murine brain capillary endothelial cells. *Exp. Cell Res.* **264:** 275–283.
26. Low, Q. E., *et al.* (2001). Wound healing in MIP-1alpha(−/−) and MCP-1(−/−) mice. *Am. J. Pathol.* **159:** 457–463.
27. Kinnula, V. L., Everitt, J. I., Whorton, A. R., and Crapo, J. D. (1991). Hydrogen peroxide production by alveolar type II cells, alveolar macrophages, and endothelial cells. *Am. J. Physiol.* **261:** L84–L91.
28. Kume, A., and Dinauer, M. C. (2000). Gene therapy for chronic granulomatous disease. *J. Lab. Clin. Med.* **135:** 122–128.
29. Reichelt, J., Bussow, H., Grund, C., and Magin, T. M. (2001). Formation of a normal epidermis supported by increased stability of keratins 5 and 14 in keratin 10 null mice. *Mol. Biol. Cell* **12:** 1557–1568.
30. Werner, S., Werner, S., and Munz, B. (2000). Suppression of keratin 15 expression by transforming growth factor β in vitro and by cutaneous injury in vivo. *Exp. Cell Res.* **254:** 80–90.
31. Hudde, T., *et al.* (2002). Modulation of hydrogen peroxide induced injury to corneal endothelium by virus mediated catalase gene transfer. *Br. J. Ophthalmol.* **86:** 1058–1062.
32. Hunt, T. K., Ellison, E. C., and Sen, C. K. (2004). Oxygen: at the foundation of wound healing—introduction. *J. World, Surg.* **28:** 291–293.
33. Arbiser, J. L., *et al.* (2002). Reactive oxygen generated by Nox1 triggers the angiogenic switch. *Proc. Natl. Acad. Sci. USA* **99:** 715–720.
34. Guan, L. M., and Scandalios, J. G. (2000). Hydrogen-peroxide-mediated catalase gene expression in response to wounding. *Free Radical Biol. Med.* **28:** 1182–1190.
35. Herbert, J. M., Bono, F., and Savi, P. (1996). The mitogenic effect of H2O2 for vascular smooth muscle cells is mediated by an increase of the affinity of basic fibroblast growth factor for its receptor. *FEBS Lett.* **395:** 43–47.
36. Pechan, P. A., Chowdhury, K., and Seifert, W. (1992). Free radicals induce gene expression of NGF and bFGF in rat astrocyte culture. *NeuroReport* **3:** 469–472.
37. Nissen, N. N., Polverini, P. J., Koch, A. E., Volin, M. V., Gamelli, R. L., and DiPietro, L. A. (1998). Vascular endothelial growth factor mediates angiogenic activity during the proliferative phase of wound healing. *Am. J. Pathol.* **152:** 1445–1452.
38. Autiero, M., Luttun, A., Tjwa, M., and Carmeliet, P. (2003). Placental growth factor and its receptor, vascular endothelial growth factor receptor-1: novel targets for stimulation of ischemic tissue revascularization and inhibition of angiogenic and inflammatory disorders. *J. Thromb. Haemostasis* **1:** 1356–1370.
39. Suzaki, Y., *et al.* (2002). Hydrogen peroxide stimulates c-Src-mediated big mitogen-activated protein kinase 1 (BMK1) and the MEF2C signaling pathway in PC12 cells: potential role in cell survival following oxidative insults. *J. Biol. Chem.* **277:** 9614–9621.

doi:10.1016/j.ymthe.2005.07.684


**40.** Hauck, C. R., Hsia, D. A., Ilic, D., and Schlaepfer, D. D. (2002). v-Src SH3-enhanced interaction with focal adhesion kinase at beta 1 integrin-containing invadopodia promotes cell invasion. *J. Biol. Chem.* **277:** 12487–12490.

**41.** Kim, J. S., *et al.* (2004). Human apolipoprotein(a) kringle V inhibits angiogenesis in vitro and in vivo by interfering with the activation of focal adhesion kinases. *Biochem. Biophys. Res. Commun.* **313:** 534–540.

**42.** Quadri, S. K., Bhattacharjee, M., Parthasarathi, K., Tanita, T., and Bhattacharya, J. (2003). Endothelial barrier strengthening by activation of focal adhesion kinase. *J. Biol. Chem.* **278:** 13342–13349.

**43.** Avraham, H. K., *et al.* (2003). Vascular endothelial growth factor regulates focal adhesion assembly in human brain microvascular endothelial cells through activation of the focal adhesion kinase and related adhesion focal tyrosine kinase. *J. Biol. Chem.* **278:** 36661–36668.

**44.** Abedi, H., and Zachary, I. (1997). Vascular endothelial growth factor stimulates tyrosine phosphorylation and recruitment to new focal adhesions of focal adhesion kinase and paxillin in endothelial cells. *J. Biol. Chem.* **272:** 15442–15451.

**45.** Hughes, P. M., Allegrini, P. R., Rudin, M., Perry, V. H., Mir, A. K., and Wiessner, C. (2002). Monocyte chemoattractant protein-1 deficiency is protective in a murine stroke model. *J. Cereb. Blood Flow Metab.* **22:** 308–317.

**46.** Salcedo, R., *et al.* (2000). Human endothelial cells express CCR2 and respond to MCP-1: direct role of MCP-1 in angiogenesis and tumor progression. *Blood* **96:** 34–40.

**47.** Crowther, M., Brown, N. J., Bishop, E. T., and Lewis, C. E. (2001). Microenvironmental influence on macrophage regulation of angiogenesis in wounds and malignant tumors. *J. Leukocyte Biol.* **70:** 478–490.

**48.** Jackson, S. H., Gallin, J. I., and Holland, S. M. (1995). The p47phox mouse knock-out model of chronic granulomatous disease. *J. Exp. Med.* **182:** 751–758.

**49.** Whitlock, B. B., *et al.* (2002). Essential role of the NADPH oxidase subunit p47(phox) in endothelial cell superoxide production in response to phorbol ester and tumor necrosis factor-alpha. *J. Biol. Chem.* **277:** 5236–5246.

**50.** Washington, E. A. (2001). Instillation of 3% hydrogen peroxide or distilled vinegar in urethral catheter drainage bag to decrease catheter-associated bacteriuria. *Biol. Res. Nurs.* **3:** 78–87.